

Pelican – a Time of Flight Cold Neutron Polarization Analysis Spectrometer at OPAL

Dehong YU*, Richard MOLE, Terry NOAKES, Shane KENNEDY and Robert ROBINSON

Bragg Institute, Australian Nuclear Science and Technology Organisation, New Illawarra Road, Lucas Heights, 2234, Australia

E-mail: dyu@ansto.gov.au

(Received December 18, 2012)

Pelican, a direct-geometry multi-purpose cold-neutron spectrometer, combines state-of-the-art monochromators and Fermi chopper systems to perform inelastic and quasi-elastic neutron scattering on a variety of materials (powder, polycrystal, single crystal, glass and liquid), covering fields of physics, chemistry and biology. The provision of cryogenic vacuum from sample to detector decreases background to a minimum level. A polarized incident beam is realized by supermirror polarizer and polarization analysis will be achieved by ^3He polarization filter. The instrument is designed to accommodate various sample environments including high magnetic fields, and low and high temperatures. Pelican is the first neutron spectrometer having a moveable high-vacuum Aluminium chamber and a full polarization analysis system.

KEYWORDS: neutron spectrometer, time of flight, cold neutrons, direct geometry, polarization, OPAL

1. Introduction

The time-of-flight direct-geometry neutron spectrometer, Pelican, has been built and installed at the OPAL research reactor, at the Australian Nuclear Science and Technology Organization (ANSTO). Pelican is to complement the rest of the neutron beam instrument suite at OPAL. The instrument is in the final stage of commissioning. The design goal was to produce a neutron spectrometer capable of simultaneous energy and polarization analysis. Such an instrument had operated for many years at the HIFAR reactor (OPAL's predecessor) in the Longpol spectrometer, which combined supermirror polarizer and analysers with beam modulation via a neutron spin flipper for energy analysis [1]. After careful consideration of key performance requirements and the opportunities provided by a new reactor and advanced beam technologies, the design concept for Pelican was based on the IN6 inelastic neutron scattering spectrometer at ILL, Grenoble, France [2], with addition of polarization analysis, large area of position-sensitive detectors and provision of cryogenic vacuum for sample and detector chambers.

The Pelican instrument was designed to meet the diverse requirements of the Australian scientific community from physics, chemistry, material science, to biology. A wide range of research fields will be covered. These include crystal-field excitations, phonon densities of states, magnetic excitations for various multifunctional materials including high T_c superconductors, novel magnetic, thermo-electric, ferroelectric and

piezoelectric materials; molecular dynamics in hydrogen-bonded and storage materials, catalytic materials, cements, soils and rocks; and water dynamics in proteins and ion diffusion in membranes. In this paper, the general design specifications of the Pelican instrument are presented, followed by descriptions of major components such as monochromator, polarizer, Fermi choppers, vacuum chambers and detector system. The evaluation of energy resolution will also be outlined.

2. Instrument Design and Selections of Major Components

2.1 Location of the Instrument

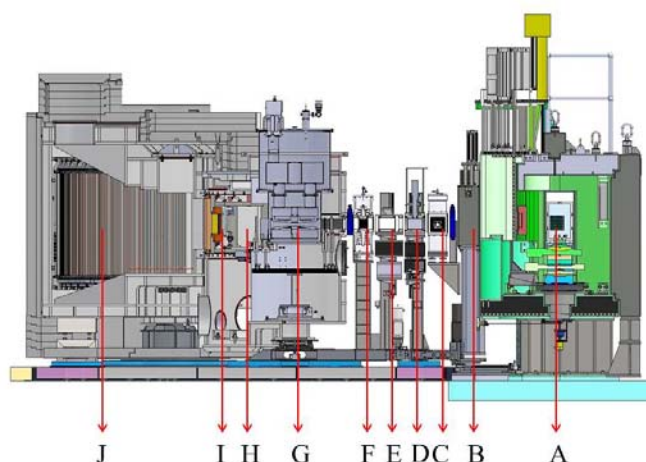
Pelican is located on the CG1 cold neutron guide, upstream of the small-angle neutron scattering instrument (Quokka) [3] in the neutron guide hall. Pelican uses the lower 15 cm of the 20 cm high neutron beam while Quokka uses the upper 5 cm. The width of the beam in the guide is 5 cm. Pelican's polished granite dance floor area is 38 m². It provides a total length of 5.4 m from the centre of the monochromator to the boundary.

2.2 General Design Specifications

Based on the scientific needs and taking into account the space restriction, the following general specifications of the instrument are defined as listed in table I. The schematic of the instrument layout is shown in Fig. 1.

Table I. General specifications of Pelican instrument

Neutron Wavelength	2.4 Å–6.3 Å, (14.2 meV–2.1 meV)
Best energy resolution	50 μeV
Q range	0.08 Å ⁻¹ – 4.5 Å ⁻¹ (elastic scatterings)
Detector solid angle	0.8 Steradians
Neutron flux at sample	2.0 × 10 ⁵ n/cm ² /s (4.0 Å tof mode)
Sample size (max.)	8 cm (H) × 3 cm (D)



Polarization analysis option is included with a solid-state supermirror to polarize the incident beam and ^3He polarizing filter for polarization analysis. Cryogenic vacuum (10^{-6} mbar) is maintained from sample region to detectors to minimize background from neutron scattering by air and any in-beam material, particularly to provide an option of doing low temperature experiments without extra vacuum shroud around the sample. $200\text{ }^3\text{He}$ position sensitive detectors, each 1 m long and 2.54 cm in diameter, achieve the desired Q and solid angle coverage.

2.3 Monochromator System

A triple monochromator system, consisting of three banks of highly oriented pyrolytic graphite (HOPG) crystals having 0.5 degree of mosaicity (ZYA), has been selected based on maximum achievable neutron flux for the designed wavelength range. There are seven crystals on each bank and they are arranged on a cam-based mechanical system to provide variable vertical focusing at the sample position. Each crystal is 2 cm high, 15 cm long and 0.13 cm thick. They are specially fabricated and optimised (Via Cordis Consulting & Movement, France) as described in reference [4]. The focusing mechanism was designed and manufactured by GAÏA, France. The crystal length of 15 cm provides large enough footprint to cover the entire width of the CG1 beam (5 cm) at low monochromator Bragg angles. This ensures efficient beam extraction for shorter wavelength settings of the spectrometer. The Bragg angle for a given neutron wavelength is defined by the middle bank, while the front and back banks have slightly different angles relative to the middle one in order to provide horizontal focusing at the sample position. The angles for the front and back banks depend on the Bragg angle of the middle one, as well as the separation between different banks and the focusing distance. With the focusing distance set at 2.69 m, the intensity at sample position was simulated with McStas [5] as a function of the separation between different banks of crystals for several different wavelengths and a compromise value of 4.5 cm was chosen. With this separation more than 98% of the maximum intensity can be achieved for the whole wavelength range as shown in Fig. 2.

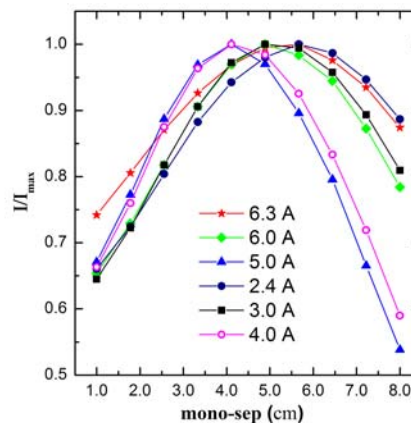


Fig. 2. Ratios of the neutron intensity I and the maximum intensity I_{max} versus monochromators separation are shown for several wavelengths.

It is noted that the simulation has taken into account the real instrument geometry, neutron source spectrum and neutron beam divergence. No extra normalization to these factors has been performed. We are only interested in the intensity variation within a small range as a function of monochromators separation.

2.4 Polarization Analysis System

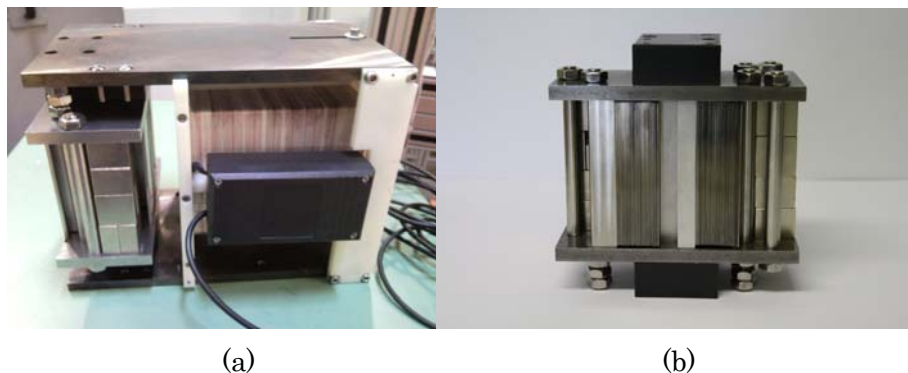


Fig. 3. The integrated polarization and spin flipper system (a) and the solid state bender-type supermirror polarizer (b) are shown.

The compact incident neutron polarization system is an integration of a solid-state bender-type supermirror polarizer with a gradient radio frequency (RF) spin flipper, as shown in Fig. 3(a), manufactured by Mirrotron Ltd. and NOB - Neutron Optics Berlin GmbH. The solid-state bender is made from silicon wafers of 0.15mm thickness coated on both sides with Fe-Si supermirrors and with $m=3$ on the outer side curvature and $m=2$ on the inner side of the curvature. Between neighbouring wafers is an absorbing layer with anti-reflection layers towards the supermirrors and a $1\mu\text{m}$ thick Gd layer in the middle to absorb the unwanted spin component. This design concept is based on that used for both polarizer and analysers on the Longpol spectrometer [6]. The overall dimensions of the bender are 105mm high, 85mm wide in the middle and 35 mm long. Due to the large width to length ratio, the bender has to be separated into three sections each having width of 28.3 mm (Fig. 3b). There is 1 degree inclination between the outer sections relative to the central section in order to match with the three individual beams from the triple monochromators. The central section is installed downstream of the outer benders for mechanical convenience. 95% polarization and 30% transmission have been achieved with this compact system for the wavelength range of $2.4 \text{ \AA} - 6.3 \text{ \AA}$. Detailed descriptions and performance of the polarization system will be presented elsewhere.

A wide-angle ^3He polarization filter will be placed after the sample for polarization analysis. The magnetic coil (*Pastis*-type [7]) and ^3He cell will be installed inside the high vacuum sample chamber through a vacuum adaptor flange. *In-situ* refilling of polarized ^3He will be implemented. Details for the ^3He polarization analysis system will be presented elsewhere.

2.4 Fermi Chopper System

Fermi chopper is selected to pulse the monochromatic neutron beams and to provide the time reference used to derive the final energies of the scattered neutrons. Two master

Table II. Fermi Chopper Specifications

Maximum Frequency	400 Hz
Phase stability	Less than 0.05%
Straight slit dimensions	
-master choppers	80 mm (H), 60 mm (W), 10 mm (L)
-slave chopper	100 mm (H), 80 mm (W), Open (no slit)
Collimations – master choppers	$1.0^\circ \pm 0.1^\circ, 2.5^\circ \pm 0.1^\circ$

Fermi choppers with different collimations have been defined for high-resolution and high-intensity applications. A further slave chopper with a large opening acts to remove frame overlap and provide an option to select a different order of diffracted neutrons from the HOPG monochromators. These choppers were manufactured by Mirrotron Ltd. and SKF Magnetic Bearings. Specifications for the Fermi chopper system are listed in table II.

The advantage of the Fermi chopper arrangement is its capability for time focusing in combination with the triple monochromators. By adjusting the frequency and the sense of rotation of the Fermi chopper, the rotating slit package can scan the monochromators in such a way to let the slow neutrons pass before the fast ones so that they arrive at the detector at same time. The time focusing frequency (Hz) is given by [8]:

$$\nu = \left[\left(L_{cs} + L_{sd} \left(\frac{\lambda_f}{\lambda_i} \right)^3 \right) \cdot \pi \cdot C \cdot \lambda_i \cdot \cot \theta \right]^{-1} \quad (1)$$

where, $L_{cs} = 0.743$ m and $L_{sd} = 2.4$ m are the distances from chopper to sample and from sample to detector respectively. λ_i and λ_f are the incident and final neutron wavelength. θ is the Bragg angle corresponding to λ_i . $C = 252.78$ $\mu s/\text{\AA}/m$, a time constant. The time focusing condition (1) can only be fulfilled for a narrow energy transfer. If we consider elastic scattering neutrons only, then we have

$$\nu = \left[(L_{cs} + L_{sd}) \cdot \pi \cdot C \cdot \lambda \cdot \cot \theta \right]^{-1} \quad (2)$$

The focusing frequency for elastic scatterings versus wavelength is shown in Fig. 4. Calculations of focusing frequency versus energy transfer for the entire wavelength range indicated that 400 Hz chopper frequency is sufficient for energy transfer up to 100 meV (neutron energy gain), as shown in Fig.5 for 5 \AA neutrons.

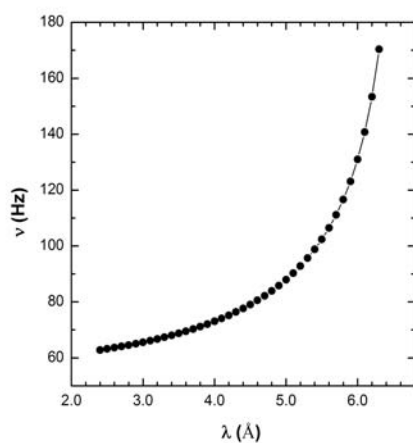


Fig. 4. Chopper focusing frequency for elastic scattering is shown as a function of wavelength.

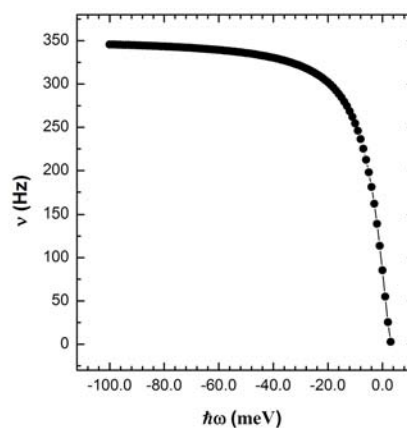


Fig. 5. Chopper focusing frequency as a function of energy transfer is shown for 5 \AA neutrons. Negative sign on the horizontal axis means neutron energy gain.

2.4 Vacuum Chambers

To minimize background from air and any in-beam material scattering, both sample and detectors are inside cryogenic vacuum chambers which are made of Aluminium. Inside the vacuum chambers are installed a radial collimator and a special designed curved isolation valve together with all associated motors, encoders, limit switches, cables and connectors. The entire internal surface is covered with 0.5 mm thick Cd. Every item inside vacuum chambers has been vacuum tested before installation. Both chambers have reached 3×10^{-6} mbar vacuum level with two turbo molecular pumps plus a *Polycold* cryogenic pump [9]. The isolation valve can maintain this vacuum level in the detector chamber when the sample chamber is under atmospheric pressure. The isolation valve is designed only to work one way with detector chamber under vacuum and sample chamber at atmospheric pressure. Its operation is controlled by a specially designed system for controlling, operating and monitoring the pumps and chamber vacuum level. The vacuum control system monitors the status of all essential parameters of vacuum pumps and issues early warnings or shuts down the whole pump system for any failure of pumps.

Outside the chambers, 100 mm thick polyethylene and 5 mm thick *RubberBore* (supplied by GAÏA, France) containing 50% B₄C are installed as the external background shielding. The total weight of the instrument is approximately 14 tons. 12 air skates are installed underneath to elevate the whole instrument for wavelength selection and instrument alignment. There are three rotation axes. The rotation around the centre of the monochromators determines the incident neutron wavelength. The rotation axis under the sample chamber aligns the detector bank with respect to sample position. The detector bank is normally positioned on the focusing configuration for improved Q resolution. However there is also an option to move the entire chamber to the opposite side (non-focusing configuration) for measurements at short wavelengths. This option was required due to space limitations when the spectrometer is set for low monochromator take-off angles. The third rotation axis pivots from the centre of the polarizer to re-align the beam at sample after the polarizer bender which deflects the beam by about 2 degrees.



Fig. 6. The 200 ³He position sensitive detectors are installed inside the detector chamber.

2.5 Detector Systems

200 ^3He position-sensitive detectors (PSD), supplied by Toshiba Electron Tubes & Devices Co., Ltd. Japan, have been installed in the detector vacuum chamber as indicated in Fig. 6. These PSDs are distributed in 25 packs each containing 8 detectors separated by a 0.5 mm thick Cd. Each individual PSD is 1 m long and 2.54 cm in diameter and filled with 10 atmosphere ^3He gas. Behind each pack is installed one Mesytec MPSD8 electronic module containing preamplifiers for 8 PSDs. The 200 detectors and 25 MPSD8 modules are operating under 3×10^{-6} mbar high vacuum. High voltage to detectors, low voltage powers to MPSD8 units and signals are feed in or out via vacuum feed-through.

To protect the PSDs from damage due to high voltage discharge in the event of vacuum breakdown, an in-house designed high-voltage protection system has been implemented. The system allows the high voltage to be on at atmospheric pressure and below 1.0×10^{-4} mbar. Note that this vacuum region is considered a safe working region for the Pelican vacuum chamber. The actual vacuum level at which discharge may occur depends on each individual case and needs to be pre-determined. Three levels of protection were built into the system. An embedded control loop will turn off the high voltage at a pre-defined rate when the vacuum deteriorates to 1.2×10^{-4} mbar. If the pressure continues to increase to 3.0×10^{-4} mbar, the analog interlock signal from the pressure measurement unit will start a soft shut down of the high voltage within 60 s. If these two protections somehow fail, the last stage will issue a hard shut down within 15 s triggered by the signal from the vacuum control system. The high-voltage protection system has been thoroughly tested.

2.5 Energy Resolution

The instrument energy resolution has been calculated as a function of neutron wavelength and energy transfer under time focusing conditions, based on the procedure outlined in [10]. The evaluation has taken into account the geometry of the instrument, mosaicity of the monochromators, sample size and detector diameter. The collimation of

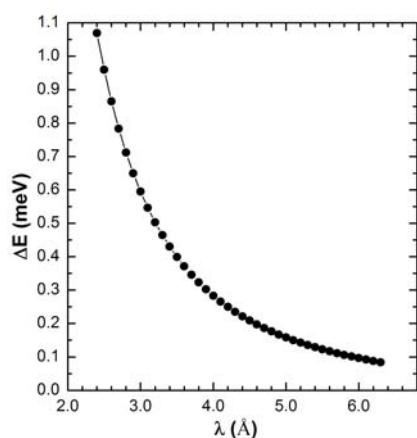


Fig. 7. Calculated elastic energy resolution as a function of wavelength is shown.

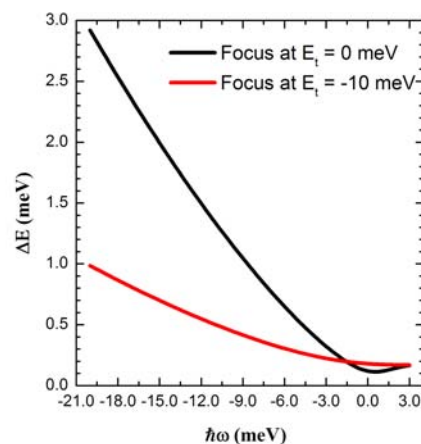


Fig. 8. Calculated energy resolution versus energy transfer is shown for 5 Å neutrons. Negative sign on the horizontal axis means energy gain.

the Fermi chopper is 1 degree. The elastic energy resolution versus neutron wavelength is shown in Fig. 7, with chopper frequency setting at the time focusing values for elastic scattered neutrons. The energy resolution as a function of energy transfer is shown in Fig. 8 for 5 Å neutrons, with time focusing setting at 0 (black) and -10 meV (red) energy transfers. It is seen that shifting the time focusing condition to -10 meV improves significantly the overall energy resolution at high energy transfer region at the cost of worsening energy resolution at the elastic peak.

3. Summary

The design of the Pelican instrument and the selection of the major components have been described. The installation has been finished and vacuum chambers have been tested. Full scale performance test is in progress and the instrument is expected to be operational in the beginning of 2014.

Acknowledgment

The authors would like to thank the technical support team at ANSTO for the great support and excellent work during the construction of the instrument. The continuing advice and encouragement from the Instrument Advisory Team members and the Project Coordination Group for the entire development period is greatly acknowledged. The thorough review of the instrument design and advice received from Dr. H. Mutka (ILL) is very much appreciated. Extensive and invaluable discussions with Dr. M. Hagen (SNS) and Prof. G. J. Kearley are gratefully acknowledged.

References

- [1] L. D. Cussen, J. C. Osborn, P. Gibbs and T. J. Hicks: Nucl. Instr. and Meth., A **314** (1992) 155.
- [2] <http://www.ill.eu/instruments-support/instruments-groups/instruments/in6/description/>
- [3] E. P. Gilbert, J. C. Schulz and T. J. Noakes: Physica B **385-386**, (2006) 1180.
- [4] A. K. Freund and D. H. Yu: Nucl. Instr. and Meth., A **634** (2011) S75.
- [5] <http://www.mcstas.org/>
- [6] Th. Krist, S. J. Kennedy, T. J. Hicks, F. Mezei: Physica B **241-242** (1998) 82.
- [7] J.R. Stewart, K.H. Andersen, E. Babcock, C.D. Frost, A. Hiess, D. Jullien, J.A. Stride, J.-F. Barthélémy, F. Marchal, A.P. Murani, H. Mutka, H. Schober: Physica B 385-386, Part 2 (2006) 1142.
- [8] H. Mutka: Nucl. Inst. and Meth. A **338** (1994) 144.
- [9] <http://www.brooks.com/>
- [10] R. Scherm, C. Carlile, J. Dianoux, J. Suck and J. White: Institut Laue-Langevin, scientific report 76S235S (1976).